

Article

## Production of Bio-Hydrogenated Diesel by Hydrotreatment of High-Acid-Value Waste Cooking Oil over Ruthenium Catalyst Supported on Al-Polyoxocation-Pillared Montmorillonite

Yanyong Liu \*, Rogelio Sotelo-Boyás, Kazuhisa Murata, Tomoaki Minowa and Kinya Sakanishi

Biomass Technology Research Center, National Institute of Advanced Industrial Science and Technology, AIST Tsukuba Center 5, 1-1-1 Higashi, Tsukuba, Ibaraki 305-8565, Japan;

E-Mails: rsotelob@gmail.com (R.S.-B.); kazu-murata@aist.go.jp (K.M.);

minowa.tom@aist.go.jp (T.M.); kinya-sakanishi@aist.go.jp (K.S.)

\* Author to whom correspondence should be addressed; E-Mail: yy.ryuu@aist.go.jp;

Tel.: +81-29-861-4826; Fax: +81-29-861-4776.

Received: 1 December 2011; in revised form: 19 January 2012 / Accepted: 7 February 2012 /

Published: 14 February 2012

---

**Abstract:** Waste cooking oil with a high-acid-value (28.7 mg-KOH/g-oil) was converted to bio-hydrogenated diesel by a hydrotreatment process over supported Ru catalysts. The standard reaction temperature, H<sub>2</sub> pressure, liquid hourly space velocity (LHSV), and H<sub>2</sub>/oil ratio were 350 °C, 2 MPa, 15.2 h<sup>-1</sup>, and 400 mL/mL, respectively. Both the free fatty acids and the triglycerides in the waste cooking oil were deoxygenated at the same time to form hydrocarbons in the hydrotreatment process. The predominant liquid hydrocarbon products (98.9 wt%) were *n*-C<sub>18</sub>H<sub>38</sub>, *n*-C<sub>17</sub>H<sub>36</sub>, *n*-C<sub>16</sub>H<sub>34</sub>, and *n*-C<sub>15</sub>H<sub>32</sub> when a Ru/SiO<sub>2</sub> catalyst was used. These long chain normal hydrocarbons had high melting points and gave the liquid hydrocarbon product over Ru/SiO<sub>2</sub> a high pour point of 20 °C. Ru/H-Y was not suitable for producing diesel from waste cooking oil because it formed a large amount of C<sub>5</sub>–C<sub>10</sub> gasoline-ranged paraffins on the strong acid sites of HY. When Al-polyoxocation-pillared montmorillonite (Al<sub>13</sub>-Mont) was used as a support for the Ru catalyst, the pour point of the liquid hydrocarbon product decreased to –15 °C with the conversion of a significant amount of C<sub>15</sub>–C<sub>18</sub> *n*-paraffins to *iso*-paraffins and light paraffins on the weak acid sites of Al<sub>13</sub>-Mont. The liquid product over Ru/Al<sub>13</sub>-Mont can be expected to give a green diesel for current diesel engines because its chemical composition and physical properties are similar to those of commercial petro-diesel. A relatively large amount of H<sub>2</sub> was consumed in the hydrogenation of unsaturated C=C bonds and the deoxygenation of C=O bonds in

the hydrotreatment process. A sulfided Ni-Mo/Al<sub>13</sub>-Mont catalyst also produced bio-hydrogenated diesel by the hydrotreatment process but it showed slow deactivation during the reaction due to loss of sulfur. In contrast, Ru/Al<sub>13</sub>-Mont did not show catalyst deactivation in the hydrotreatment of waste cooking oil after 72 h on-stream because the waste cooking oil was not found to contain sulfur-containing compounds.

**Keywords:** bio-hydrogenated diesel; waste cooking oil; hydrotreatment; ruthenium; Al-polyoxocation; pillared montmorillonite

---

## 1. Introduction

The increase of environmental concerns and the depletion of petroleum reserves have stimulated the search for alternative renewable fuels to avoid climate change and energy shortage [1]. Bio-diesel, which has been recognized as “green fuel”, is an important alternative fuel made from renewable resources such as vegetable oil [2]. Although bio-diesel is a renewable fuel with environmental benefits, the utilization of nonfood biomass is important from the viewpoint of food supply [3]. Waste cooking oil is an important biomass resource without competition from food uses [4]. It is presumed that 100–140 kt waste cooking oil from the household sector is discarded every year in Japan [5]. Recently the production of bio-diesel from waste cooking oil has been studied worldwide [6–9].

Fatty acid methyl ester (FAME) is the first generation bio-diesel and it is produced by the transesterification of vegetable oil with methanol [10]. However, FAME has some shortcomings as a fuel for the current diesel engines because both C=C bonds and C=O bonds remain in the molecules of FAME [11]. The anti-oxidation ability of FAME is low due to unsaturated C=C double bonds, and the flash point of FAME is high as FAME is less flammable than paraffins.

Bio-hydrogenated diesel (abbreviated as BHD) is called the second generation bio-diesel and it is produced by the hydrotreatment of vegetable oil, instead of the transesterification of vegetable oil [12]. BHD is a paraffin mixture because all unsaturated C=C double bonds have been hydrogenated and all oxygen atoms have been eliminated in the hydrotreatment process.

The waste cooking oil usually contains a high concentration of free fatty acids, which greatly increase the cost in the production of FAME type bio-diesel. Base catalysts are highly active in the transesterification of triglycerides with methanol to produce FAME. However, base catalysts lose their activity in the transesterification of high-acid-value waste cooking oil as they react with free fatty acids to form soap. Acid-catalyzed transesterification is much slower than base-catalyzed although some new acid catalysts have been developed [6]. In general, a complex two-step process has to be used for the FAME production from high-acid-value waste cooking oil: using acid catalysts to convert free fatty acids in the first step and base catalysts to convert triglycerides in the second step. On the other hand, the conversion of high-acid-value waste cooking oil to hydrocarbon type bio-diesel has an economical advantage in that both free fatty acids and triglycerides are deoxygenated at the same time in a one-step hydrotreatment process [13].

Although vegetable oil can be converted to a mixture of paraffins, cycloparaffins, and aromatic hydrocarbons at high temperatures under high pressures even without a catalyst, a relatively large

amount of fatty acids usually remain in the products [14]. Solid acid catalysts (such as H-ZSM-5,  $\text{SO}_4/\text{ZrO}_2$ , *etc.*) can convert vegetable oil to a mixture of gasoline, kerosene, light gas oil, gas oil, and long chain residues by the hydrotreatment process [9,15]. Industrial FCC catalysts can convert vegetable oil to gasoline distilled hydrocarbons in the FCC unit under the FCC conditions [16]. For converting vegetable oil to bio-hydrogenated diesel (BHD), two types of effective catalysts have been reported for the hydrotreatment process: noble metal catalysts (Pd, Pt, *etc.*) [17–21], and desulfurized catalysts (sulfided Ni-Mo, Co-Mo, Ni-W, Co-W, *etc.*) [21–24].

The yield of  $\text{C}_{15}$ – $\text{C}_{18}$  *n*-paraffins usually has been stated in the literature for the hydrotreatment of vegetable oil and it seems that the amount of  $\text{C}_{15}$ – $\text{C}_{18}$  *n*-paraffins determines the quality of BHD fuel [18–22]. Actually, an extreme amount of  $\text{C}_{15}$ – $\text{C}_{18}$  *n*-paraffins give BHD a low fluidity and hinder the use of BHD in current diesel engines. Any post-treatments in adapting BHD for current diesel engines would increase the cost of BHD production. We think that the character of commercial normal diesel from crude oil should be used as a goal for BHD because the current diesel engines have been designed to use normal diesel as a fuel [23]. We have combined sulfided Ni-Mo and solid acids to adjust the composition and properties of BHD in the hydrotreatment of vegetable oils [23,24]. However, the sulfided Ni-Mo catalyst slowly deactivated during the reaction because of sulfur loss [24]. Ru has been reported as an effective noble metal catalyst for desulfurization [25]. Clays are sorts of solid acids with a porous structure and unique acidity [26,27]. Pillaring large metal polyoxocations (such as  $[\text{AlO}_4\text{Al}_{12}(\text{OH})_{24}(\text{H}_2\text{O})_{12}]^{7+}$ ) into the interlayer region of clays (such as montmorillonite) increases the surface area, pore size, and temperature stability of clay materials [27]. Al-polyoxocation-pillared montmorillonite has been reported as an excellent catalyst for producing diesel distilled hydrocarbons from heavy vacuum gas oil and Fischer-Tropsch wax by the hydrotreatment process [28,29].

In this study, we combined Ru with Al-polyoxocation-pillared montmorillonite to convert high-acid-value waste cooking oil to BHD for current diesel engines by the hydrotreatment process, as compared with other supports ( $\text{SiO}_2$  and H-Y zeolite) and metal catalyst (sulfided Ni-Mo).

## 2. Experimental Section

### 2.1. Materials

Waste vegetable cooking oil was obtained from a restaurant (served fried chicken) and used without any purification. The standard reagents of fatty acids and triglycerides were purchased from Sigma-Aldrich Chemical Company (St. Louis, MO, USA) and Tokyo Kasei Chemical Company (Tokyo, Japan). Chemical reagents for synthesizing catalysts were purchased from Wako Pure Chemical Industries Company (Tokyo, Japan).

Na-type montmorillonite (denoted as Na-Mont) is a natural clay mineral (Kunipia F) supplied by Kunimine Industrial Company (Tokyo, Japan). The cation exchange capacity (CEC) was about 100 meq/100 g and the particle size was smaller than 2  $\mu\text{m}$  in the Na-Mont sample. Na-Y zeolite ( $\text{SiO}_2/\text{Al}_2\text{O}_3 = 5.5$ ; BET surface area:  $382 \text{ m}^2\cdot\text{g}^{-1}$ ) was purchased from Wako Pure Chemical Industries Company (Tokyo, Japan).  $\text{SiO}_2$  support (BET surface area:  $300 \text{ m}^2\cdot\text{g}^{-1}$ ; average pore size: 10 nm) were purchased from Fuji Silysia Chemical Company (Tokyo, Japan).

## 2.2. Catalysts

[AlO<sub>4</sub>Al<sub>12</sub>(OH)<sub>24</sub>(H<sub>2</sub>O)<sub>12</sub>]<sup>7+</sup>-pillared montmorillonite (denoted as Al<sub>13</sub>-Mont) was prepared by ion-exchange [30,31]. The pillaring solution of [AlO<sub>4</sub>Al<sub>12</sub>(OH)<sub>24</sub>(H<sub>2</sub>O)<sub>12</sub>]<sup>7+</sup> was prepared by the dropwise addition of a solution of 0.2 M NaOH (2.4 g NaOH in 300 mL H<sub>2</sub>O) to a solution of 0.5 M Al(NO<sub>3</sub>)<sub>3</sub> (9.38 g Al(NO<sub>3</sub>)<sub>3</sub>·9H<sub>2</sub>O in 50 mL H<sub>2</sub>O) until a OH/Al molar ratio of 2.4. After standing at room temperature for 24 h, 5 g Na-Mont was added to the pillaring solution. The final suspension was stirred at room temperature for 12 h and a solid sample was obtained by filtration. The solid sample was washed with distilled water three times, dried at 100 °C for 24 h, and calcined at 400 °C for 3 h.

H-Y was prepared from Na-Y by ion-exchange. Na-Y was stirred in an aqueous solution of NH<sub>4</sub>NO<sub>3</sub> (0.1 M) for 3 h and NH<sub>4</sub>-Y was then obtained after filtering from the water. The obtained NH<sub>4</sub>-Y was dried at 100 °C for 24 h and calcined at 550 °C for 3 h to form H-Y.

Ru-supported catalysts (Ru/SiO<sub>2</sub>, Ru/H-Y, and Ru/Al<sub>13</sub>-Mont) were synthesized using a wet impregnation method. The calcined solid support (SiO<sub>2</sub>, H-Y, or Al<sub>13</sub>-Mont) was impregnated with an aqueous solution of RuCl<sub>3</sub>·*n*H<sub>2</sub>O (Ru: 40.6 wt%) with stirring. A solid sample was obtained after evaporating the water by heating at 90 °C. The obtained solid sample was dried at 100 °C for 24 h and calcined at 400 °C for 3 h. The designed Ru loading was 1.0 wt% in each catalyst because 5 g solid support and 0.124 g RuCl<sub>3</sub>·*n*H<sub>2</sub>O (Ru: 40.6 wt%) in 50 mL water were used for the catalyst preparation. The actual Ru loadings, which were measured by ICP elemental analysis, were similar to the designed Ru loadings in various catalysts. Prior to the reaction, the catalysts were reduced in a H<sub>2</sub> flow (flow rate: 60 mL·min<sup>-1</sup>) at 350 °C for 2 h.

Ni-Mo/Al<sub>13</sub>-Mont was synthesized as a reference catalyst using a co-impregnation method [31,32]. Al<sub>13</sub>-Mont support was added to a mixed aqueous solution of (NH<sub>4</sub>)<sub>6</sub>Mo<sub>7</sub>O<sub>24</sub>·4H<sub>2</sub>O and Ni(NO<sub>3</sub>)<sub>2</sub>·6H<sub>2</sub>O to form a slurry. The slurry was stirred at 90 °C until formation of a solid sample by evaporating water. The obtained solid sample was dried at 100 °C for 24 h and calcined at 400 °C for 3 h. The loadings of MoO<sub>3</sub> and NiO were 15 wt% and 3 wt% in Ni-Mo/Al<sub>13</sub>-Mont, respectively. Prior to the reaction, the catalyst was sulfided and reduced in a mixed gas containing 10% H<sub>2</sub>S and 90% H<sub>2</sub> (flow rate: 60 mL·min<sup>-1</sup>) at 400 °C for 10 h.

## 2.3. Characterization

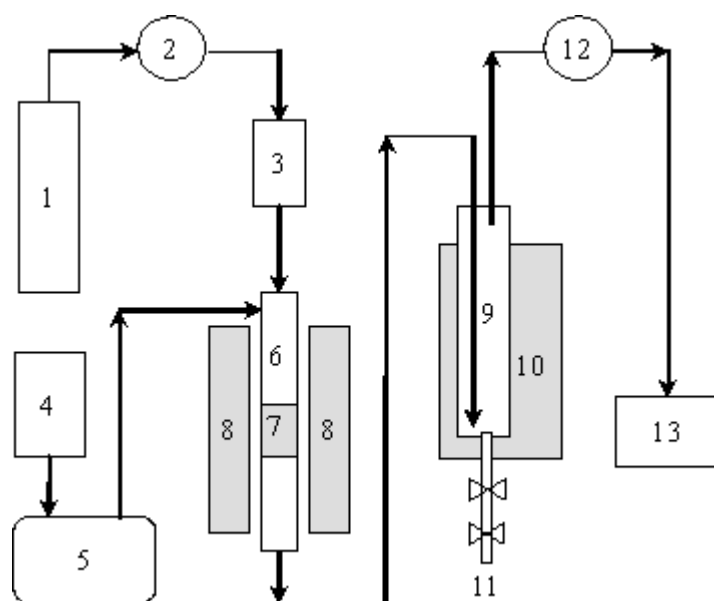
The elemental composition of waste cooking oil was determined using an elemental analyzer (CE instrument EA1110). The chemical composition of waste cooking oil was analyzed using an Agilent 6890 N FID-GC with an Omnistar Q-mass. A HP-624 capillary column was used to separate free fatty acids and an UA-TRG capillary column was used to separate triglycerides, diglycerides, and monoglycerides. The density of waste cooking oil was determined at 20 °C using a density/specific gravity meter (Kyoto Electronics DA-130N). The viscosity of waste cooking oil was determined at 40 °C using a vibro viscometer (A&D Co. Lim., Tokyo, Japan, SV-10). The acid value of waste cooking oil was determined by an acid-base titration technique using a KOH aqueous solution (ASTM D 664). The limit of detection was 0.1 mg-KOH/g-liquid in the measurement of the acid value. Iodine values of the oils were measured by a titration technique using ICl and Na<sub>2</sub>S<sub>2</sub>O<sub>3</sub> solutions (ASTM D 1959).

Transmission electron microscopy (TEM) images were obtained using a JEOL JEM 2010FX electron microscope equipped with a Hitachi/Keveo H-8100/Delta IV EDS operating at 200 kV. The *ex situ* treated samples were supported on Mo grids for the observations. The powder X-ray diffraction (XRD) patterns were measured using a MAC Science MXP-18 diffractometer with Cu K $\alpha$  radiation operating at 40 kV and 50 mA. Temperature-programmed desorption of ammonia (NH<sub>3</sub>-TPD) was carried out using a BELCAT-B automatic system equipped with a TCD and an Omnistar Q-mass. A part of the 0.05 g sample was pretreated at 400 °C for 1 h in a He flow with a flow rate of 50 mL·min<sup>-1</sup>. After the temperature was decreased to 100 °C, ammonia was adsorbed onto the sample's surface, followed by evacuation for 1 h at 100 °C to eliminate the weakly adsorbed ammonia. Then, NH<sub>3</sub>-TPD was recorded from 100 to 600 °C with a rate of 8 °C·min<sup>-1</sup>.

#### 2.4. Reaction

A high-pressure continuous flow fixed-bed reactor was used for the experimental investigation. Figure 1 shows the reaction system used in this study. A stainless steel tubular reactor (*i.d.*: 1 cm; length: 50 cm) was used for loading the catalyst and a furnace was used for heating the tubular reactor. The waste cooking oil was forced into the reactor at a constant rate by a JP-H type high-pressured micro-feeder (Furue Science Company). Meanwhile, a mixed gas containing 90% H<sub>2</sub> and 10% Ar (using as an internal standard) was introduced into the reactor from a high-pressure H<sub>2</sub> cylinder and the flow rate was controlled by a mass flow controller. A cooling trap (put in ice-water) was set between the reactor exit and the back-pressure regulator to collect liquid products. The catalyst was loaded onto an iron plate with many small holes in the center of the tubular reactor. The pressure in the reaction system was controlled by a back-pressure regulator. The reaction

**Figure 1.** Reaction system used in this study. (1) H<sub>2</sub> cylinder; (2) pressure regulator; (3) mass flow controller; (4) tank of waste cooking oil; (5) high-pressured micro-feeder; (6) stainless steel tubular reactor; (7) catalyst layer; (8) furnace; (9) cold trap; (10) tank of ice-water; (11) outlet of liquid product; (12) back-pressure regulator; (13) on-line GCs.



The catalyst was loaded onto an iron plate with many small holes in the center of the tubular reactor. The pressure in the reaction system was controlled by a back-pressure regulator. The reaction

temperature was controlled by a temperature-controller equipped with a thermocouple. The top of the thermocouple was in contact with the surface of the catalyst layer to determine the reaction temperature. The standard reaction conditions were listed as follows: catalyst amount: 1 g (mixed with quartz sand to 5 mL in total volume); reaction temperature: 350 °C; H<sub>2</sub> pressure: 2 MPa; LHSV (liquid hourly space velocity, which is a ratio of the volume of liquid feed to the volume of catalyst and quartz sand): 15.2 h<sup>-1</sup>; ratio of H<sub>2</sub> to oil in feed: 400 mL/mL, in which the H<sub>2</sub> volume was described in the conditions of standard temperature and pressure (STP).

### 2.5. Analyses

The gas products were continuously analyzed by an on-line GC system during the reaction. Inorganic gases (H<sub>2</sub>, Ar, CO and CO<sub>2</sub>) were analyzed using a Shimadzu 8A TCD-GC equipped with MS-5A and Porapak-Q columns. Gaseous hydrocarbons (C<sub>1</sub>–C<sub>4</sub>) were analyzed using an Agilent 6890 N FID-GC equipped with a RT-QPLOT capillary column. The factors of various gases were obtained using a standard mixed gas (with known concentration for each component) from a cylinder.

The liquid products were taken out from the cooling trap after the reaction. After removing the water layer in the bottom using a separation funnel, a certain amount of 1-methylnaphthalene was added to the oil phase as an internal standard. The oil phase was then analyzed by an Agilent 6890 N FID-GC equipped with three capillary columns: a UA-DX30 capillary column for analyzing C<sub>5+</sub> hydrocarbons, a HP-624 capillary column for analyzing fatty acids, and a UA-TRG capillary column for analyzing triglycerides, diglycerides, and monoglycerides.

The yields of C<sub>1</sub>–C<sub>4</sub> hydrocarbons, CO and CO<sub>2</sub> in the gas products were calculated using Ar as internal standard. The yields of organic compounds in the liquid products were calculated using 1-methylnaphthalene as internal standard. The yield of water was calculated from the weights of formed water and introduced oil. The carbon mass balance had an error <5% over each catalyst.

## 3. Results and Discussion

### 3.1. Characterization of Catalysts

Table 1 summarizes the basic characteristics of the Na-Mont and Al<sub>13</sub>-Mont before and after calcination. The value of the basal plane reflection ( $d_{001}$ ) at the lowest angle in the XRD pattern includes the thickness of a host layer and the gallery height of an interlayer region [26,33]. Because the interlayer cations support the montmorillonite layers, any alternations of interlayer cations certainly cause changes of the  $d_{001}$  basal plane in the XRD pattern. The thickness of the host layer is about 9.3 Å for montmorillonite compounds [26,27]. As shown in Table 1, the  $d_{001}$  basal plane at 25 °C in the XRD pattern increased from 12.4 Å to 19.2 Å after Al<sub>13</sub> polyoxocation pillaring. After subtracting the thickness of the host layer (9.3 Å) from the  $d_{001}$  spacing, Na-Mont had a gallery height of 3.1 Å and Al<sub>13</sub>-Mont had a gallery height of 9.9 Å. The Al<sub>13</sub> polyoxocations were successfully introduced into the interlayer region in Al<sub>13</sub>-Mont because the gallery height coincided with the size of Al<sub>13</sub> polyoxocation [26,27]. The  $d_{001}$  value of Na-Mont decreased to 10.6 Å after calcination at 300 °C for 3 h and could not be observed after calcination at 500 °C for 3 h.

**Table 1.** Basic characteristics of raw montmorillonite and its Al<sub>13</sub>-pillared derivative.

Sample	$T_{\text{calcination}}$ (°C)	$d_{001}$ (Å)	BET (m <sup>2</sup> /g)	Total $V_p$ (cm <sup>3</sup> /g)	Micro $V_p$ (cm <sup>3</sup> /g)
Na-Mont	25	12.4	82	0.079	0.004
	300	10.6	38	0.068	0.005
	400	10.5	29	0.065	0.004
	500	–	26	0.063	0.003
Al <sub>13</sub> -Mont	25	19.2	156	0.150	0.078
	300	18.5	237	0.170	0.111
	400	18.5	270	0.180	0.122
	500	17.9	189	0.152	0.103

As shown in Table 1, the BET surface area of Al<sub>13</sub>-Mont was significantly higher than that of its precursor Na-Mont at 25 °C. The height between two clay layers in Na-Mont was only 3.1 Å (from XRD results) and many water molecules existed in the interlayer region at 25 °C. Hence, the interior of the interlayer region in Na-Mont was difficult to utilize for adsorbing N<sub>2</sub> molecules in the BET measurement. On the other hand, the gallery height of Al<sub>13</sub>-Mont increased to 9.9 Å (from XRD results) and thus N<sub>2</sub> molecules easily enter the interlayer region, which caused a significant increase of BET surface area of Al<sub>13</sub>-Mont at 25 °C. Moreover, the BET surface area of Na-Mont decreased to 38 m<sup>2</sup>/g after calcination at 300 °C for 3 h due to the collapse of the layered structure. On the other hand, the  $d_{001}$  value of Al<sub>13</sub>-Mont slightly decreased to 18.5 Å upon calcination at 300 °C due to the dehydration of Al<sub>13</sub> polyoxocation. The BET surface area of Al<sub>13</sub>-Mont increased with increasing calcination temperature up to 400 °C, followed by a decrease of surface area upon calcination at 500 °C. Hence, Al<sub>13</sub>-Mont retained the layered structures after calcination at 400 °C owing to the robust polyoxocation pillars but were partly destroyed upon calcination at 500 °C. As for the pore size of a montmorillonite compound, it is defined not only by the interlayer distance (between two clay layers) but also by the lateral distance (between two interlayer pillars). The micropore (pores diameter <20 Å) volume of Na-Mont was very low (about 0.004 cm<sup>3</sup>/g). On the other hand, Al<sub>13</sub>-Mont is a mesoporous material because its micropore volume is relatively large. Both the total pore volume and the micropore volume of Al<sub>13</sub>-Mont increased with increasing calcination temperature up to 400 °C and decreased upon calcination at 500 °C due to partial destruction of the layered structure. Therefore, the calcination temperature for Al<sub>13</sub>-Mont-containing catalysts was set at 400 °C in this study.

Figure 2 shows the TEM image of Ru/Al<sub>13</sub>-Mont (Ru loading: 1 wt%) catalyst after reduction in a H<sub>2</sub> flow at 300 °C for 2 h. The layered structure of montmorillonite support could be observed from the TEM image. The gallery height was about 1 nm and this value coincided with the size of Al<sub>13</sub> polyoxocation. The black Ru particles could be observed on the surface of the montmorillonite support. The Ru particles did not enter into the interlayer region of montmorillonite in Ru/Al<sub>13</sub>-Mont. The distribution of Ru particles was relatively uniform and the particle size of Ru was about 3–5 nm.

**Figure 2.** TEM image of Ru/Al<sub>13</sub>-Mont (Ru loading: 1 wt%) catalyst after reduction.

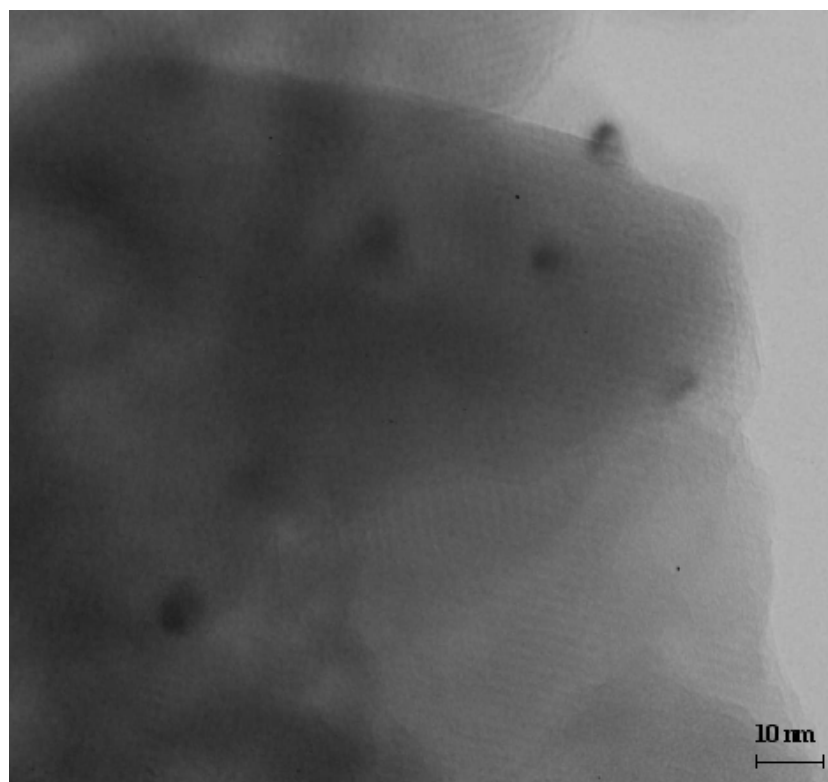


**Figure 3.** NH<sub>3</sub>-TPD profiles of various solid supports.

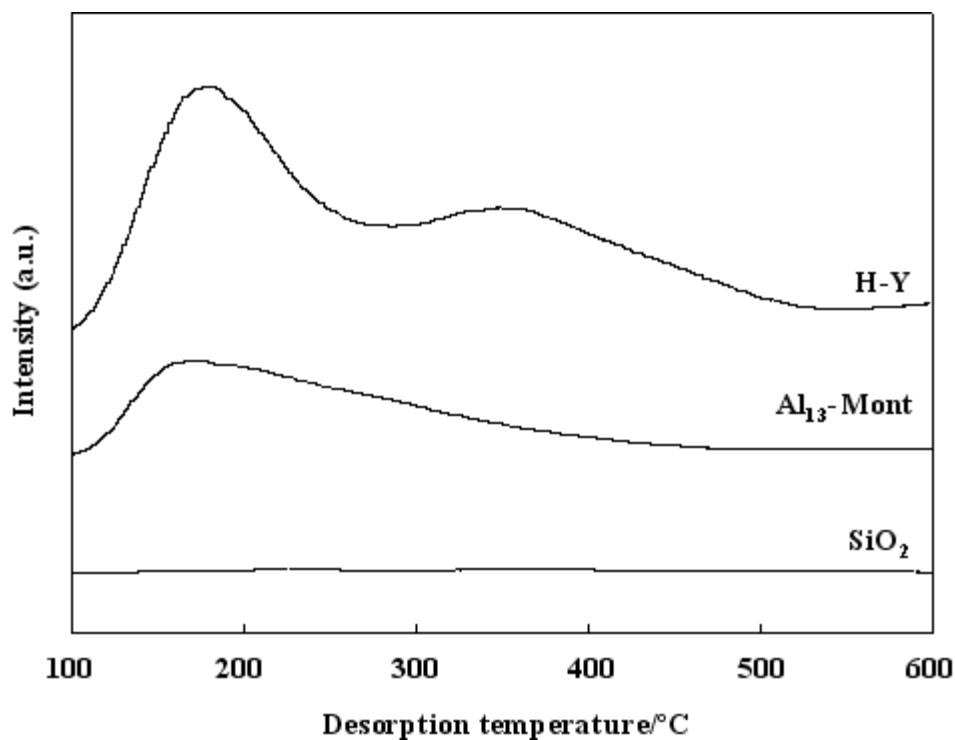


Figure 3 shows the NH<sub>3</sub>-TPD of various solid supports used in this study. NH<sub>3</sub>-TPD is a powerful tool for estimating the acidic property of a solid surface. The adsorbed NH<sub>3</sub> molecules desorbed from weak acid sites at low temperatures and desorbed from strong acid sites at high temperatures. As shown in Figure 3, SiO<sub>2</sub> did not show an obvious peak in the NH<sub>3</sub>-TPD profile, indicating that SiO<sub>2</sub>

did not have acid sites on the surface. Al<sub>13</sub>-Mont had acid sites on the surface area because its NH<sub>3</sub>-TPD showed a peak with a maximum value at 170 °C. Because H-Y showed two peaks at about 180 and 350 °C, H-Y had two types of acid sites (weak acid sites and strong acid sites) on the surfaces. The peak at the maximum temperature in the NH<sub>3</sub>-TPD profile corresponds to the strongest acid sites on the solid surface. The nature of a solid acid catalyst is mainly determined by the strongest acid sites on the surface. According to the peak position at the maximum temperature in the NH<sub>3</sub>-TPD profiles, the acidic strength of various supports was in an order of H-Y > Al<sub>13</sub>-Mont > SiO<sub>2</sub> (no acidity).

### 3.2. Composition and Property of Waste Cooking Oil

Table 2 shows the composition and property of the waste cooking oil used in this study.

**Table 2.** Composition and property of the waste cooking oil used in this study.

<b>Elemental composition</b>	C	H	N	S	O
<b>Weight percent (wt%)</b>	77.91	11.69	0.04	0	10.36
<b>Chemical composition</b>	Triglyceride	Diglyceride	Monoglycerid	Free fatty acid	
<b>Content (g/100 g-oil)</b>	79.1	1.8	2.2	16.9	
<b>Others</b>	Acid value (mg-KOH/g-oil)	Iodine value (g-I <sub>2</sub> /100 g-oil)	Viscosity (mPa/s)	Density (g/mL)	
	28.7	88.6	57.8	0.92	

The elemental composition of the waste cooking oil was determined using an elemental analyzer (CE instrument EA1110). The difference from 100% was taken as the content of oxygen. As shown in Table 2, the amount of N was very small (0.04 wt%) and S could not be observed in the waste cooking oil. In general, vegetable oils do not contain sulfur-containing compounds. Therefore, the bio-diesels produced from vegetable oils are regarded as environmentally benign green fuels. Concurrently, the development of catalysts for the hydrotreatment of vegetable oils (without S) is different from those for the hydrotreatment of fossil fuels with sulfur-containing compounds.

The chemical components in the waste cooking oil were confirmed by GC-MS results and standard reagents. The content of free fatty acids was very high (16.9 g/100 g-oil) in the waste cooking oil. It seems that the waste cooking oil can not be used as a straight vegetable oil (SVO) just after filtration because the free fatty acids are corrosive to diesel engines. For the FAME production, base catalysts lose their activity in the transesterification of cooking vegetable oil because of soap formation from free fatty acids and basic catalysts. A complex two-step process has to be used for the FAME production (using acid catalyst to convert free fatty acids in the first step and using base catalyst to convert triglycerides in the second step) which must increase the cost of the FAME production. Therefore, the one-step hydrotreatment process is suitable for the commercial production of BHD from waste cooking oil.

As for the physical properties, the acid value of the waste cooking oil was very high (28.7 mg-KOH/g-oil) because it contained a large amount of free fatty acids. The iodine value of the waste cooking oil was 88.6 g-I<sub>2</sub>/100 g-oil, indicating that the waste cooking oil contained many C=C unsaturated bonds. The viscosity at 30 °C was 57.8 mPa/s and the density at 25 °C was 0.92 g/mL for the waste cooking oil. The viscosity was too high to use the waste cooking oil in current diesel engines.

Table 3 shows the species of free fatty acid (FFA) in the waste cooking oil used in this study. The formula of each fatty acid was confirmed by GC-MS (HP-624 capillary column) results with standard reagents. The content of each fatty acid shown in Table 3 was expressed as its weight in 100 g free fatty acid, while 100 g waste cooking oil contained 16.9 g free fatty acid (Table 2). The main free fatty acids in the waste cooking oil were palmitic acid (6.6%), stearic acid (7.8%), oleic acid (53.6%), linoleic acid (16.4%), and linolenic acid (14.3%). The unsaturated fatty acids (with C=C double bond) included palmitoleic, oleic, linoleic, linolenic, and eicosenoic acids, while the saturated fatty acids (without C=C double bond) included palmitic and stearic acids. By calculating using these data, the unsaturated fatty acids occupied 85.6% and the saturated fatty acids occupied 14.4% in total free fatty acids of the waste cooking oil. All free fatty acids in the waste cooking oil had even carbon numbers (16, 18, and 20) in the carbon chains. The fatty acids with sixteen carbons in the carbon chain (so-called C<sub>16</sub>-acids, including palmitic and palmitoleic acids) occupied 6.8%, the fatty acids with eighteen carbons in the carbon chain (so-called C<sub>18</sub>-acids, including stearic, oleic, linoleic and linolenic acids) occupied 92.1%, and the fatty acids with twenty carbons in the carbon chain (so-called C<sub>20</sub>-acids, including eicosenoic acid) occupied 1.1% in total free fatty acids of the waste cooking oil.

**Table 3.** Species of free fatty acid (FFA) in the waste cooking oil used in this study.

Formula	Name	Structure <sup>a</sup>	Content (g/100 g-FFA)
C <sub>16</sub> H <sub>32</sub> O <sub>2</sub>	Palmitic	C16:0	6.6
C <sub>16</sub> H <sub>30</sub> O <sub>2</sub>	Palmitoleic	C16:1	0.2
C <sub>18</sub> H <sub>36</sub> O <sub>2</sub>	Stearic	C18:0	7.8
C <sub>18</sub> H <sub>34</sub> O <sub>2</sub>	Oleic	C18:1	53.6
C <sub>18</sub> H <sub>32</sub> O <sub>2</sub>	Linoleic	C18:2	16.4
C <sub>18</sub> H <sub>30</sub> O <sub>2</sub>	Linolenic	C18:3	14.3
C <sub>20</sub> H <sub>38</sub> O <sub>2</sub>	Eicosenoic	C20:1	1.1

<sup>a</sup> C<sub>x</sub>:y, where x is the number of carbon atoms and y is the number of C=C double bonds.

### 3.3. Hydrotreatment of Waste Cooking Oil over Ru-Supported Catalysts

Table 4 shows the product yields over various catalysts in the hydrotreatment of waste cooking oil. The conversion was 100% and did not decrease after reaction for 10 h over each catalyst because triglycerides and fatty acid acids could not be detected in the products. The yield of fuel gas (C<sub>1</sub> + C<sub>2</sub>) was very low (<1.0 wt%) over each catalyst. The yield of liquid fuel (C<sub>5+</sub> hydrocarbons) was in a narrow range of 82.1–84.0 wt% and the yield of LPG (C<sub>3</sub> + C<sub>4</sub>) was in a narrow range of 4.8–5.6 wt% over each catalyst. Both liquid hydrocarbons (C<sub>5+</sub>) and LPG (C<sub>3</sub> + C<sub>4</sub>) can be used as fuels for automobiles. Water (yield: 7.7–8.0 wt%) and CO<sub>x</sub> (including CO and CO<sub>2</sub>, yield: 3.2–3.4 wt%) were also formed in the hydrotreatment process over each catalyst. Because propane is formed after all C=O bonds in triglycerides are broken during the hydrotreatment process, propane occupied more than 90 wt% in the formed LPG (C<sub>3</sub> + C<sub>4</sub>) over each catalyst.

**Table 4.** Product yields over various catalysts in the hydrotreatment of waste cooking oil <sup>a</sup>.

Catalyst	C <sub>1</sub> + C <sub>2</sub>	C <sub>3</sub> + C <sub>4</sub>	C <sub>5+</sub>	CO <sub>x</sub>	H <sub>2</sub> O
Ru/SiO <sub>2</sub>	0.2	4.8	84.0	3.3	7.7
Ru/Al <sub>13</sub> -Mont	0.4	5.0	83.6	3.2	7.8
Ru/H-Y	0.9	5.6	82.1	3.4	8.0

<sup>a</sup> Reaction temperature: 350 °C; H<sub>2</sub> pressure: 2 MPa; H<sub>2</sub>/oil in feed: 400 mL/mL; LHSV: 15.2 h<sup>-1</sup>.

The waste cooking oil contained triglycerides, diglycerides, monoglycerides, and free fatty acids (Table 2). The hydrotreatment process on the Ru sites contained two steps: hydrogenation and deoxygenation. In the first step, all unsaturated C=C bonds in the triglycerides, diglycerides, monoglycerides, and free fatty acids were saturated on their carbon chains by the hydrogenation on the Ru sites. In the second step, the saturated triglycerides decomposed by scission of the C=O bonds, leading to the formation of diglycerides, monoglycerides, and carboxylic acids (fatty acids) in order, and the carboxylic acids then underwent deoxygenation on the Ru sites to form hydrocarbons. Therefore, the key step in the hydrotreatment of waste cooking oil is the deoxygenation of saturated fatty acids.

The deoxygenation of saturated fatty acids (such as stearic acid C<sub>17</sub>H<sub>35</sub>COOH) contains three parallel reactions: reduction, decarbonylation, and decarboxylation [22].



As shown in Reactions 1–3, for a fatty acid with an even carbon number, the reduction produces a normal paraffin with an even carbon number plus water; the decarbonylation produces a normal paraffin with an odd carbon number plus water and CO; and the decarboxylation produces a normal paraffin with an odd carbon number plus CO<sub>2</sub>. Both the decarbonylation and the decarboxylation occurred during the reaction because both CO and CO<sub>2</sub> were detected in the gas product over each catalyst.

As shown in Table 4, the three catalysts had similar yields of C<sub>5+</sub> liquid hydrocarbons (ranging from 82.1 to 84.0 wt%) from the hydrotreatment of waste cooking oil. However, it is necessary to investigate whether these liquid hydrocarbons are suitable for use as a diesel fuel in current diesel engines.

Figure 4 shows the FID-GC charts (UA-DX capillary column) of liquid hydrocarbons formed from the hydrotreatment of waste cooking oil over various catalysts. Ru/SiO<sub>2</sub> formed *n*-C<sub>18</sub>H<sub>38</sub>, *n*-C<sub>17</sub>H<sub>36</sub>, *n*-C<sub>16</sub>H<sub>34</sub>, and *n*-C<sub>15</sub>H<sub>32</sub> as the main products and the amounts of *iso*-paraffins and light paraffins (≤C<sub>14</sub>) were very low. According to Reactions 1–3, *n*-C<sub>16</sub>H<sub>34</sub> and *n*-C<sub>18</sub>H<sub>38</sub> were formed by the reduction of palmitic acid and stearic acid, and *n*-C<sub>15</sub>H<sub>32</sub> and *n*-C<sub>17</sub>H<sub>36</sub> were formed by the decarbonylation and decarboxylation of palmitic acid and stearic acid, respectively. In order to adjust the chemical composition of the liquid hydrocarbon product, we supported Ru catalyst on solid acids (H-Y, Al<sub>13</sub>-Mont) for the isomerization/cracking of C<sub>15</sub>H<sub>32</sub>–C<sub>18</sub>H<sub>38</sub> *n*-paraffins as the third step after the hydrogenation and deoxygenation steps. The isomerization/cracking of *n*-paraffins over bifunctional catalysts containing metal and solid acid is very important for improving the properties of liquid hydrocarbon fuels [34–37]. The reaction proceeds via carbenium ion intermediates formed on the solid acid sites. The acidic strength of the solid acid determines the activity of the bifunctional catalysts

when the same metal is used in the isomerization/cracking of *n*-paraffins. Because the acidic strength of various supports was in the order of H-Y > Al<sub>13</sub>-Mont > SiO<sub>2</sub> (Figure 3), Ru/H-Y formed a large amount of light hydrocarbons ( $\leq C_{14}$ ) and Ru/Al<sub>13</sub>-Mont formed a significant amount of light hydrocarbons ( $\leq C_{14}$ ) (Figure 4).

**Figure 4.** FID-GC charts of liquid hydrocarbons formed from the hydrotreatment of waste cooking oil over various catalysts (reaction conditions: same as those in Table 4).

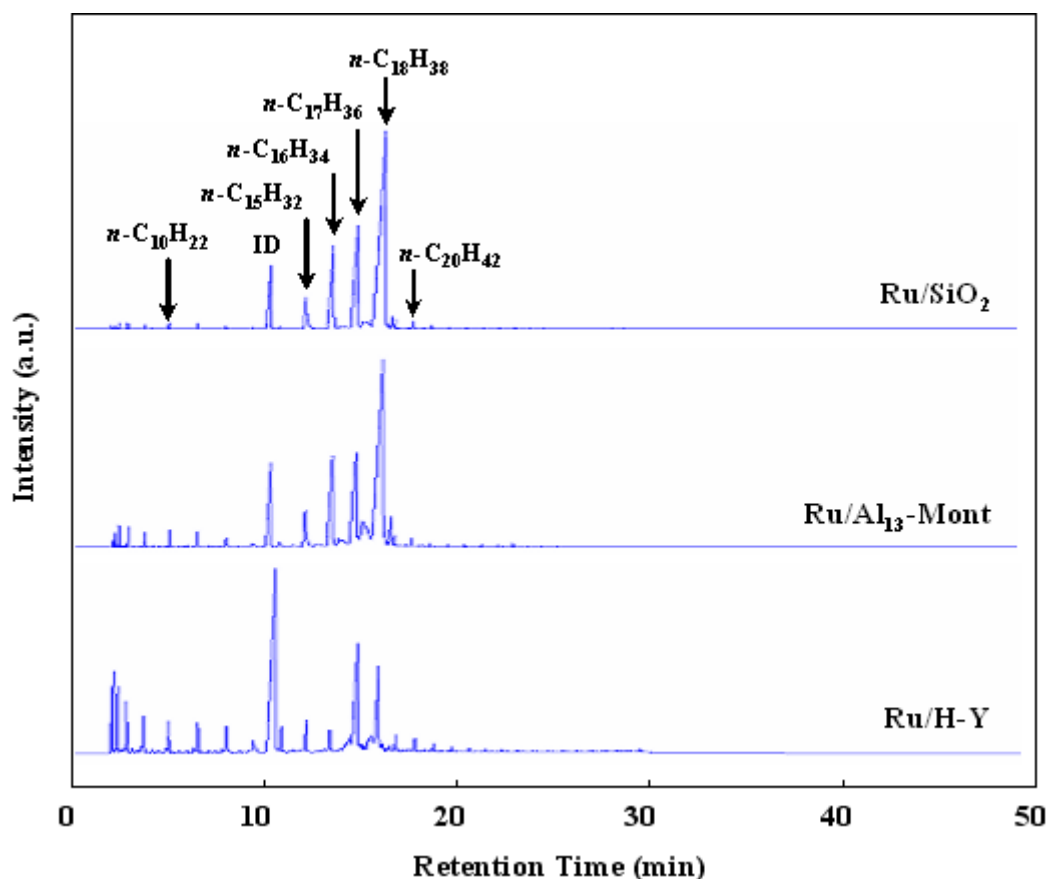


**Table 5.** Composition and property of the liquid hydrocarbons (C<sub>5+</sub>) formed from the hydrotreatment of waste cooking oil over various catalysts <sup>a</sup>.

Catalyst	Composition (wt%)			Property			
	C <sub>5</sub> –C <sub>10</sub>	C <sub>11</sub> –C <sub>20</sub>	C <sub>20+</sub>	Iso/n ratio	Pour Point (°C)	Density at 25 °C (g/mL)	Viscosity at 30 °C (mPa/s)
Ru/SiO <sub>2</sub>	0.9	98.9	0.2	0.08	20	0.79	8.01
Ru/Al <sub>13</sub> -Mont	9.1	89.8	1.1	0.22	–15	0.78	3.96
Ru/H-Y	42.8	56.5	0.7	0.43	— <sup>b</sup>	0.77	2.08
Normal diesel <sup>c</sup>	8.2	88.1	3.7	0.28	–15	0.82	3.69

<sup>a</sup> Reaction temperature: 350 °C; H<sub>2</sub> pressure: 2 MPa; H<sub>2</sub>/oil in feed: 400 mL/mL; LHSV: 15.2 h<sup>–1</sup>; <sup>b</sup> Lower than –25 °C; <sup>c</sup> A commercial diesel bought from a petrol station.

Table 5 shows the composition and property of the liquid hydrocarbons (C<sub>5+</sub>) formed from the hydrotreatment of waste cooking oil over various catalysts. Although the liquid hydrocarbons formed over Ru/SiO<sub>2</sub> contained the largest amount of C<sub>11</sub>–C<sub>20</sub> diesel-distillate (98.9 wt%) with the lowest

*iso/n* ratio (0.08) among various catalysts, the pour point of the product was too high (20 °C) to use as a diesel fuel. Ru/H-Y was also not suitable for producing BHD from the waste cooking oil because it formed a large amount of C<sub>5</sub>–C<sub>10</sub> gasoline-distillate (42.8 wt%) on the strong acid sites. Ru/Al<sub>13</sub>-Mont produced a liquid hydrocarbon product with a pour point of –15 °C with an *iso/n* ratio of 0.22.

The melting points of *n*-C<sub>18</sub>H<sub>38</sub>, *n*-C<sub>17</sub>H<sub>36</sub>, *n*-C<sub>16</sub>H<sub>34</sub>, and *n*-C<sub>15</sub>H<sub>32</sub> are 28, 22, 18, and 10 °C, respectively. A predominant amount of C<sub>15</sub>–C<sub>18</sub> *n*-paraffins gave a high pour point (20 °C) for the liquid hydrocarbon product over Ru-Mo/SiO<sub>2</sub> (Table 5). It is necessary to decrease the pour point of the product over Ru/SiO<sub>2</sub> in order to use it in the current diesel engines. *Iso*-paraffins and light paraffins have relatively low melting points (for example, 2-methyl-heptadecane: 5 °C; 3-methyl-heptadecane: –6 °C; 2-methyl-hexadecane: 5 °C; 2-methyl-pentadecane: –11 °C; 3-methyl-pentadecane: –22 °C; 2-methyl-tetradecane: –8 °C; 3-methyl-tetradecane: –36 °C; *n*-C<sub>11</sub>H<sub>24</sub>: –25 °C). Hence, we supported Ru on solid acids (Al<sub>13</sub>-Mont and H-Y) to improve the fluidity of the liquid hydrocarbon product from the hydrotreatment of waste oil by the isomerization/cracking of C<sub>15</sub>H<sub>32</sub>–C<sub>18</sub>H<sub>38</sub> *n*-paraffins.

The hydrocarbons ranging from C<sub>11</sub> to C<sub>20</sub> are called diesel-distillate and the hydrocarbons ranging from C<sub>5</sub> to C<sub>10</sub> are called gasoline-distillate. However, the commercial normal diesel bought from a petrol station actually contains 8.2 wt% of C<sub>5</sub>–C<sub>10</sub> gasoline-distillate to improve the fluidity (Table 5). The viscosity of the liquid hydrocarbon product over Ru/Al<sub>13</sub>-Mont was 3.96 mPa/s, which was quite similar to that of the normal diesel (3.69 mPa/s). The density of the normal diesel was relatively large (0.82 g/mL), probably because the normal diesel contained some heavy additives. On the whole, both composition and pour point of the liquid hydrocarbon product over Ru/Al<sub>13</sub>-Mont were quite similar to those of the normal diesel bought from a petrol station. Because the current diesel engines have been designed to use normal diesel as a fuel, we think that the product over Ru/Al<sub>13</sub>-Mont (with similar composition and property to normal diesel) is better than the product over Ru/SiO<sub>2</sub> (with 98.9 wt% C<sub>11</sub>–C<sub>20</sub> diesel-distillate and high pour point) as a diesel fuel for current diesel engines. As a result, because Al<sub>13</sub>-Mont had a significant acidic strength, the liquid hydrocarbon product in the hydrotreatment of waste cooking oil over Ru/Al<sub>13</sub>-Mont can be expected to give a green BHD fuel directly usable in the current diesel engines without any post-treatment processes (such as distillation, upgrading, *etc.*).

#### 3.4. Influence of Reaction Conditions in the Hydrotreatment of Waste Cooking Oil over Ru/Al<sub>13</sub>-Mont

Because the molecules of triglycerides and free fatty acids in the waste cooking oil contained many unsaturated C=C bonds and C=O bonds, the H<sub>2</sub> amount and H<sub>2</sub> pressure are important reaction conditions for the hydrotreatment of waste cooking oil to produce saturated hydrocarbons.

Figure 5 shows the effect of H<sub>2</sub>/oil ratio in the hydrotreatment of waste cooking oil over Ru/Al<sub>13</sub>-Mont. The H<sub>2</sub>/oil was a ratio of H<sub>2</sub> feed rate to liquid (waste cooking oil) feed rate during the reaction and the H<sub>2</sub> volume was described in conditions of standard temperature and pressure (STP). A low H<sub>2</sub>/oil is desirable for producing BHD for commercialization as it is favorable to reduce the cost of production. However, the peaks of fatty acids could be detected in the GC chart at a H<sub>2</sub>/oil ratio of 300 (Figure 5). Thus a H<sub>2</sub>/oil ratio of 400 was necessary for the hydrotreatment of waste cooking oil over Ru/Al<sub>13</sub>-Mont. As shown in Reactions 1–3, the deoxygenation of fatty acids contained three parallel reactions: reduction, decarbonylation and decarboxylation. The reduction does not produce CO<sub>x</sub>, while

both the decarbonylation and the decarboxylation produces  $\text{CO}_x$  and thus one C in the carbon chain is lost. Thus from the deoxygenation of  $\text{C}_{16}$ -acids and  $\text{C}_{18}$ -acids, the reduction produces  $n\text{-C}_{16}\text{H}_{34}$  and  $n\text{-C}_{18}\text{H}_{38}$ , and the decarbonylation and decarboxylation produce  $n\text{-C}_{15}\text{H}_{32}$  and  $n\text{-C}_{17}\text{H}_{36}$ . Moreover, the reduction is favorable under a large  $\text{H}_2/\text{oil}$  ratio because it consumes more  $\text{H}_2$  molecules than the decarbonylation and decarboxylation (Reactions 1–3). Hence, the ratios of  $\text{C}_{18}/\text{C}_{17}$  and  $\text{C}_{16}/\text{C}_{15}$  in products over Ru/Al<sub>13</sub>-Mont decreased with decreasing  $\text{H}_2/\text{oil}$  ratio from 500 to 300 (Figure 5).

**Figure 5.** FID-GC charts of liquid products in the hydrotreatment of waste cooking oil over Ru/Al<sub>13</sub>-Mont under various  $\text{H}_2/\text{oil}$  ratios ( $T$ : 350 °C;  $\text{H}_2$  pressure: 2 MPa; liquid hourly space velocity (LHSV): 15.2 h<sup>-1</sup>).

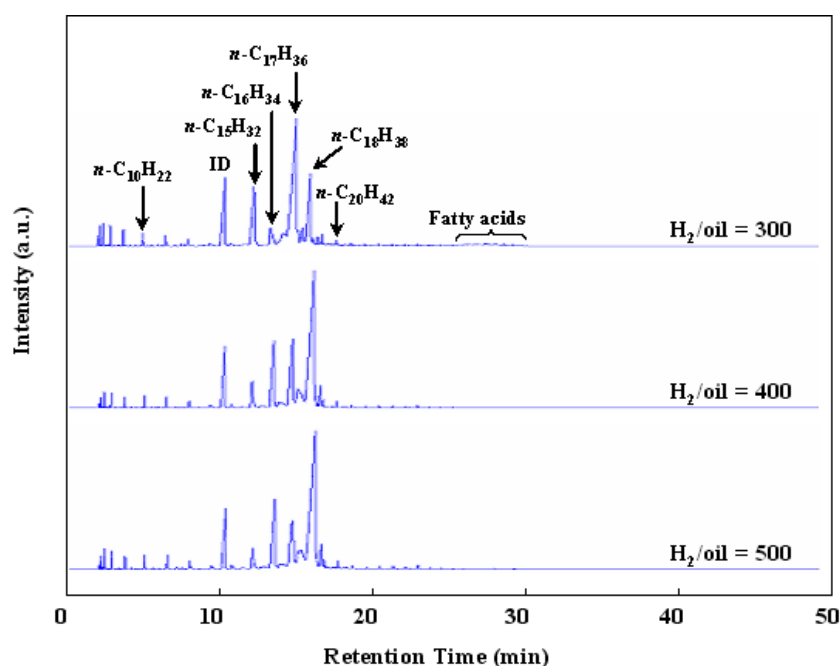


**Figure 6.** FID-GC charts of liquid products in the hydrotreatment of waste cooking oil over Ru/Al<sub>13</sub>-Mont under various  $\text{H}_2$  pressures ( $T$ : 350 °C;  $\text{H}_2/\text{oil}$ : 400; LHSV: 15.2 h<sup>-1</sup>).

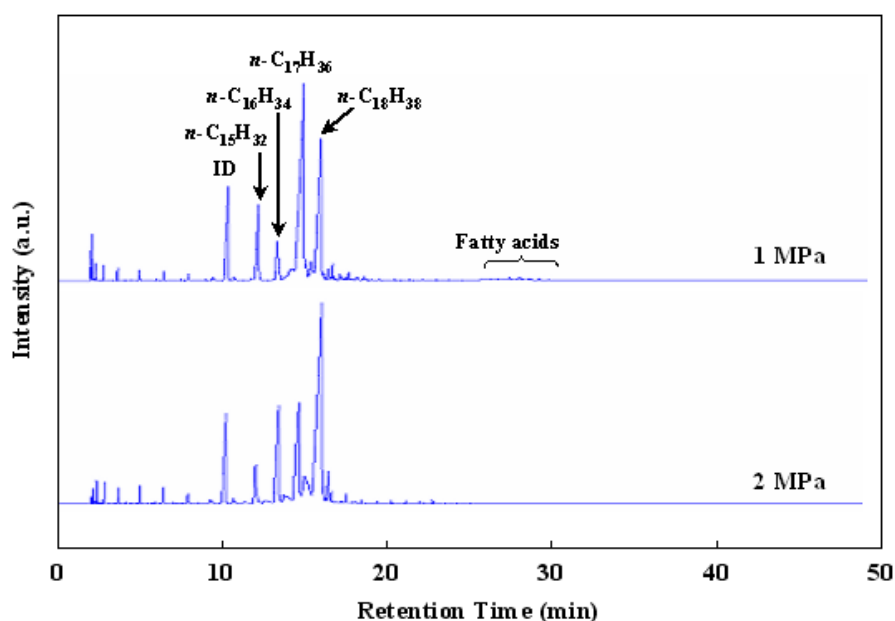
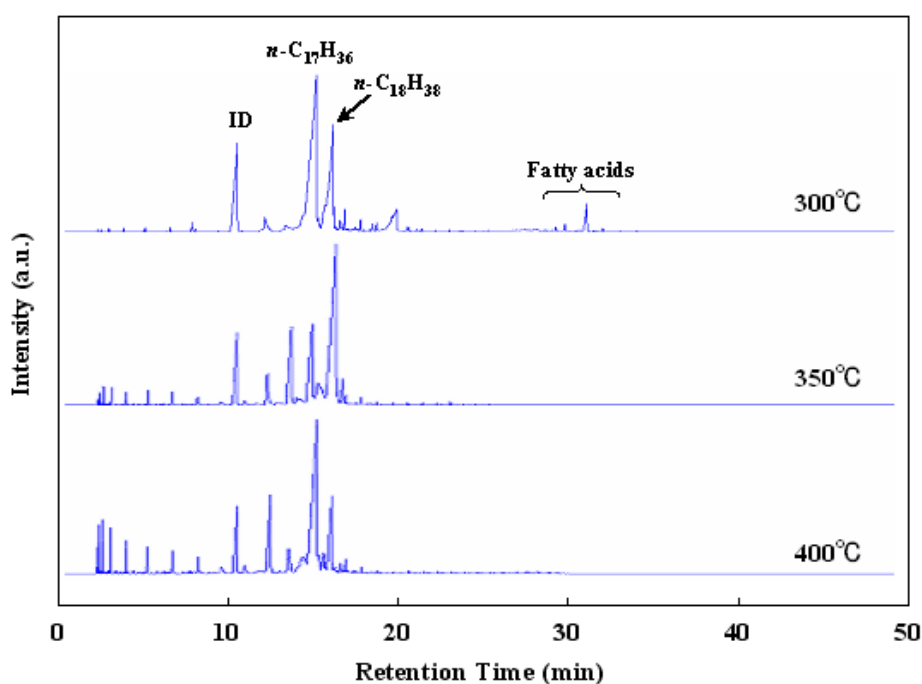


Figure 6 shows the effect of H<sub>2</sub> pressure in the hydrotreatment of waste cooking oil over Ru/Al<sub>13</sub>-Mont. A low H<sub>2</sub> pressure is desirable for producing BHD in commercialization because it is favorable to reduce the investment in plant and equipment. The peaks of fatty acids could not be observed in the GC chart under 2 MPa of H<sub>2</sub> pressure but could be detected in the GC chart under 1 MPa of H<sub>2</sub> pressure. Hence, a H<sub>2</sub> pressure of 2 MPa was necessary for the hydrotreatment of waste cooking oil over Ru/Al<sub>13</sub>-Mont. As shown in Reactions 1–3, the reduction (for producing *n*-C<sub>18</sub>H<sub>38</sub> and *n*-C<sub>16</sub>H<sub>34</sub>) is favorable under a high H<sub>2</sub> pressure in comparison with the decarbonylation and decarboxylation (for producing *n*-C<sub>17</sub>H<sub>36</sub> and *n*-C<sub>15</sub>H<sub>32</sub>). Thus the ratios of C<sub>18</sub>/C<sub>17</sub> and C<sub>16</sub>/C<sub>15</sub> in products over Ru/Al<sub>13</sub>-Mont decreased with decreasing H<sub>2</sub> pressure.

Figure 7 shows the effect of reaction temperature in the hydrotreatment of waste cooking oil over Ru/Al<sub>13</sub>-Mont. When the reaction was carried out at a low reaction temperature of 300 °C, the peaks of fatty acids were observed in the GC chart. This means that the deoxygenation of waste cooking oil was not enough at 300 °C. The peaks of fatty acids could not be observed in GC charts at high reaction temperatures of 350 °C and 400 °C. Although *n*-C<sub>18</sub>H<sub>38</sub>, *n*-C<sub>17</sub>H<sub>36</sub>, *n*-C<sub>16</sub>H<sub>34</sub>, and *n*-C<sub>15</sub>H<sub>32</sub> are the main products over all three catalysts, the amount of light hydrocarbons (≤C<sub>14</sub>) formed remarkably increased when the reaction temperature increased from 300 to 400 °C. We think the cracking of C<sub>15</sub>H<sub>32</sub>–C<sub>18</sub>H<sub>38</sub> normal paraffins caused the increase of light hydrocarbons (≤C<sub>14</sub>) at high reaction temperatures. Hence, the reaction temperature also can be used to adjust the composition and property of the BHD product. Because the amount of C<sub>5</sub>–C<sub>10</sub> gasoline-distillate hydrocarbons was too much at 400 °C, the most suitable reaction temperature was found to be 350 °C in the hydrotreatment of waste cooking oil.

**Figure 7.** FID-GC charts of liquid products in the hydrotreatment of waste cooking oil over Ru/Al<sub>13</sub>-Mont at various reaction temperatures (H<sub>2</sub> pressure: 2 MPa; H<sub>2</sub>/oil: 400; LHSV: 15.2 h<sup>-1</sup>).



The goal of this study is to produce green BHD fuel for use in current diesel engines without any post-treatment. The liquid organic phase in the product should not contain any fatty acids because they

are corrosive to engines. Moreover, a significant amount of  $C_5$ – $C_{10}$  gasoline-distillate (similar to the amount in commercial normal diesel) should be contained in order to adjust the physical properties of BHD fuel to fit current diesel engines. Hence, we chose a  $H_2$ /oil ratio of 400 mL/mL, a  $H_2$  pressure of 2 MPa, and a reaction temperature of 350 °C as the standard reaction conditions in this study.

### 3.5. Deactivation of Ru/Al<sub>13</sub>-Mont and Sulfided Ni-Mo/Al<sub>13</sub>-Mont Catalysts

Figure 8 shows the time sequences in the hydrotreatment of waste cooking oil over Ru/Al<sub>13</sub>-Mont and sulfided Ni-Mo/Al<sub>13</sub>-Mont. Ru/Al<sub>13</sub>-Mont showed an initial  $C_{5+}$  hydrocarbons yield of 83.6% and it did not decrease after reaction for 72 h. This indicated that Ru/Al<sub>13</sub>-Mont had a high catalytic stability for the hydrotreatment of waste cooking oil. In contrast, sulfided Ni-Mo/Al<sub>13</sub>-Mont showed an initial  $C_{5+}$  hydrocarbons yield of 83.5% but it slowly decreased to 76.8% after reaction for 72 h. Ni-Mo/Al<sub>13</sub>-Mont was sulfided by 10%  $H_2S$  (in 90%  $H_2$ ) at 400 °C prior to the reaction and a Ni-Mo-S phase was formed as the active phase for the hydrotreatment of waste cooking oil. The sulfur component in sulfided Ni-Mo/Al<sub>13</sub>-Mont was lost slowly during the reaction [24]. Because the waste cooking oil used in this study did not contain a sulfur component (Table 2), the loss of sulfur could not be supplemented by the feedstock. As shown in Figure 8, the speed of deactivation was slow in the first 10 h and became fast after reaction for 10 h over sulfided Ni-Mo/Al<sub>13</sub>-Mont. The loss of sulfur caused the collapse of the Ni-Mo-S active phase in sulfided Ni-Mo/Al<sub>13</sub>-Mont. As for Ru/Al<sub>13</sub>-Mont, it could maintain activity during the reaction because the feedstock did not contain any sulfur poisons.

**Figure 8.** Time courses in the hydrotreatment of waste cooking oil over Ru/Al<sub>13</sub>-Mont (●) and sulfided Ni-Mo/Al<sub>13</sub>-Mont (■) (reaction conditions: same as those in Table 4).

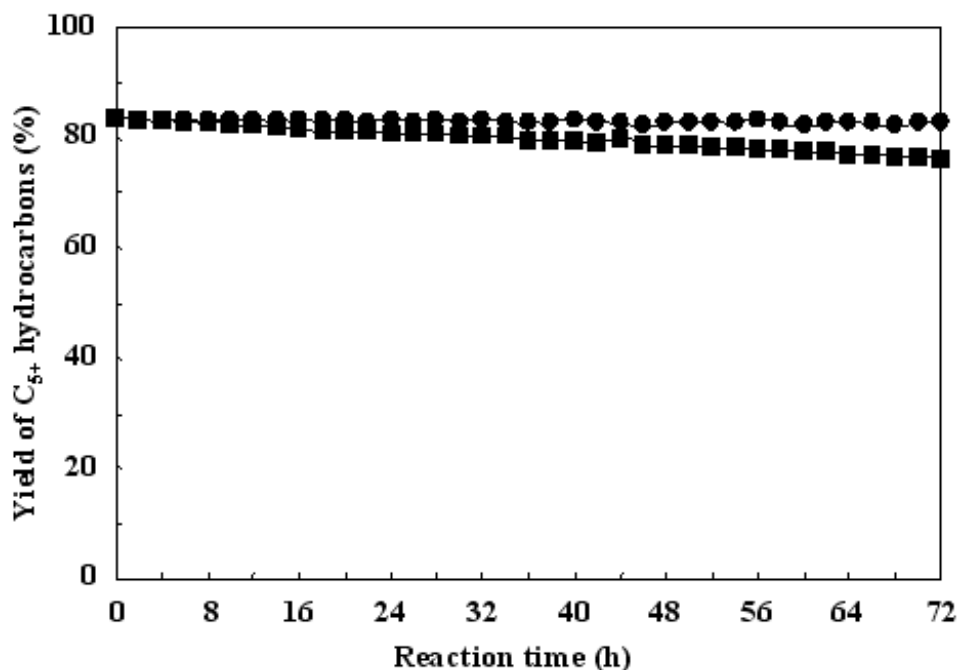
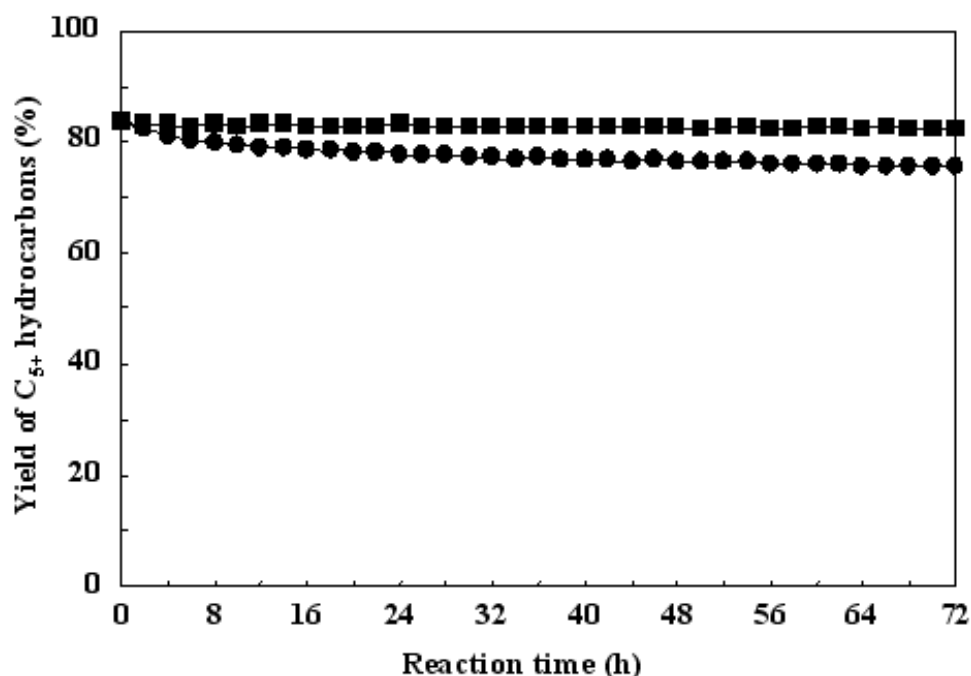


Figure 9 shows the time sequences in the hydrotreatment of waste cooking oil containing 10 ppm dimethyl disulfide (DMDS) over Ru/Al<sub>13</sub>-Mont and sulfided Ni-Mo/Al<sub>13</sub>-Mont. A large number of liquid fuels produced from crude oil, coal, and biomass contain sulfur compounds. We added 10 ppm

DMDS as a standard sulfur compound in the waste cooking oil to check the influence of sulfur on Ru/Al<sub>13</sub>-Mont and sulfided Ni-Mo/Al<sub>13</sub>-Mont catalysts. As shown in Figure 9, Ru/Al<sub>13</sub>-Mont showed an initial C<sub>5+</sub> hydrocarbons yield of 83.6% and it decreased to 75.8% after reaction for 72 h for the hydrotreatment of waste cooking oil containing 10 ppm DMDS. Because S rapidly reacted with the Ru atoms to form an inactive RuS phase on the catalyst surface, the speed of deactivation over Ru/Al<sub>13</sub>-Mont was fast in the first 10 h and then became slow. In contrast, sulfided Ni-Mo/Al<sub>13</sub>-Mont showed an initial C<sub>5+</sub> hydrocarbons yield of 83.5% and it did not decrease after reaction for 72 h. The sulfur compound (DMDS) in the feed waste cooking oil supplemented the loss of sulfur from the surface of sulfided Ni-Mo/Al<sub>13</sub>-Mont catalyst. The structure the Ni-Mo-S active phase remained during the reaction and maintained the catalytic activity of sulfided Ni-Mo/Al<sub>13</sub>-Mont. Some researchers have carried out the hydrotreatment of vegetable oil (not containing S) mixed with heavy vacuum oil (containing S) over Ni-Mo catalysts in order to maintain the catalyst stability [22]. Hence, in the hydrotreatment process, noble catalysts (Ru, Pt, Pd, *etc.*) are suitable for the feedstock without a S component (such as vegetable oils, F-T waxes, *etc.*), and desulfurized catalysts (sulfided Ni-Mo, Co-Mo, Ni-W, Co-W, *etc.*) are suitable for the feedstock containing S compounds (such as heavy oil, bio oil, *etc.*).

**Figure 9.** Time sequences in the hydrotreatment of waste cooking oil containing 10 ppm DMDS over Ru/Al<sub>13</sub>-Mont (●) and sulfided Ni-Mo/Al<sub>13</sub>-Mont (■) (reaction conditions: same as those in Table 4).



#### 4. Conclusions

The waste cooking oil containing 16.9 wt% free fatty acids was converted to mixed paraffins over Ru-supported catalysts by a one-step hydrotreatment process in which both free fatty acids and triglycerides were deoxygenated at the same time. The fluidity of the liquid hydrocarbon product over Ru/SiO<sub>2</sub> was poor because of a predominant amount of C<sub>15</sub>H<sub>32</sub>–C<sub>18</sub>H<sub>38</sub> *n*-paraffins. By supporting Ru

on acidic Al<sub>13</sub>-Mont, both the chemical composition and the pour point of the liquid hydrocarbon product became quite similar to those of a commercial normal diesel. Ru/Al<sub>13</sub>-Mont acted as a multifunctional catalyst enabling hydrogenation, deoxidization, and isomerization/cracking for the hydrotreatment of waste cooking oil. The lowest H<sub>2</sub>/oil ratio was 400 and the lowest H<sub>2</sub> pressure was 2 MPa to convert the waste cooking oil to saturated hydrocarbons over Ru/Al<sub>13</sub>-Mont as the waste cooking oil contained many unsaturated C=C bonds and C=O bonds. Ru/Al<sub>13</sub>-Mont did not deactivate after reaction for 72 h because the waste cooking oil did not contain S compounds as poisons for Ru.

## References

1. Fernando, S.; Adhikari, S.; Chandrapal, C.; Murali, N. Biorefineries: Current status, challenges, and future direction. *Energy Fuel* **2006**, *20*, 1727–1737.
2. Sharma, Y.C.; Singh, B.; Upadhyay, S.N. Advancements in development and characterization of biodiesel: A review. *Fuel* **2008**, *87*, 2355–2373.
3. Pinzi, S.; Garcia, L.; Lopez-Gimenez, F.J.; Luque de Castro, M.D.; Dorado, G.; Dorado, M.P. The ideal vegetable oil-based biodiesel composition: A review of social, economical and technical implications. *Energy Fuel* **2009**, *23*, 2325–2341.
4. Kulkarni, M.G.; Dalai, A.K. Waste cooking oil—An economical source for biodiesel: A review. *Ind. Eng. Chem. Res.* **2006**, *45*, 2901–2913.
5. Japanese government biomass policies: Major source of introduction of biofuel. *Report on Promotion of Eco-Fuel for Transportation*; Japanese Government: Tokyo, Japan, 2006.
6. Cao, F.; Chen, Y.; Zhai, F.; Li, J.; Wang, J.; Wang, X.; Wang, S.; Zhu, W. Biodiesel production from high acid value waste frying oil catalyzed by superacid heteropolyacid. *Biotechnol. Bioeng.* **2008**, *101*, 93–100.
7. Toba, M.; Abe, Y.; Kuramochi, H.; Osako, M.; Mochizuki, T.; Yoshimura, Y. Hydrodeoxygenation of waste vegetable oil over sulfide catalysts. *Catal. Today* **2011**, *164*, 533–537.
8. Xu, J.; Xiao, G.; Zhou, Y.; Jiang, J. Production of biofuels from high-acid-value waste oils. *Energy Fuel* **2011**, *25*, 4638–4642.
9. Charusiri, W.; Vitidsant, T. Kinetic study of used vegetable oil to liquid fuels over sulfated zirconia. *Energy Fuel* **2005**, *19*, 1783–1789.
10. Ma, F.; Hanna, M.M. Biodiesel production: A review. *Bioresour. Technol.* **1999**, *70*, 1–15.
11. Sharma, Y.C.; Singh, B.; Upadhyay, S.N. Advancements in development and characterization of biodiesel: A review. *Fuel* **2008**, *87*, 2355–2373.
12. Kalnes, T.; Markery, T.; Shonnard, D.R. Green diesel: A second generation biofuel. *Int. J. Chem. React. Eng.* **2007**, *5*, A48.
13. Guzman, A.; Torres, J.E.; Prada, L.P.; Nunez, M.L. Hydropressing of crude palm oil at pilot plant scale. *Catal. Today* **2010**, *156*, 38–43.
14. Li, L.; Coppola, E.; Rine, J.; Miller, J.L.; Walker, D. Catalytic hydrothermal conversion of triglycerides to non-ester biofuels. *Energy Fuel* **2010**, *24*, 1305–1315.
15. Charusiri, W.; Vitidsant, T. Catalytic cracking of used cooking oil to liquid fuels over HZSM-5. *J. Energy* **2003**, *5*, 58–68.

16. Melero, J.A.; Clavero, M.M.; Calleja, G.; Garcia, A.; Miravalles, R.; Galindo, T. Production of biofuels via the catalytic cracking of mixtures of crude vegetable oils and nonedible animal fats with vacuum gas oil. *Energy Fuel* **2010**, *24*, 707–717.
17. Maki-Arvela, P.; Kubickova, I.; Snare, M.; Eranen, K.; Murzin, D.Y. Catalytic deoxygenation of fatty acids and their derivatives. *Energy Fuel* **2007**, *21*, 30–41.
18. Maki-Arvela, P.; Rozmyszowicz, B.; Lestari, S.; Simakova, O.; Eranen, K.; Salmi, T.; Murzin, D.Y. Catalytic deoxygenation of tall oil fatty acid over palladium supported on mesoporous carbon. *Energy Fuel* **2011**, *25*, 2815–2825.
19. Murata, K.; Liu, Y.; Inaba, M.; Takahara, I. Production of synthetic diesel by hydrotreatment of Jatropha oils using Pt-Re/H-ZSM-5 catalyst. *Energy Fuel* **2010**, *24*, 2404–2409.
20. Wildschut, J.; Mahfud, F.H.; Venderbosch, R.H.; Heeres, H.J. Hydrotreatment of fast pyrolysis oil using heterogeneous noble-metal catalysts. *Ind. Eng. Chem. Res.* **2009**, *48*, 10324–10334.
21. Sotelo-Boyás, R.; Liu, Y.; Minowa, T. Renewable diesel production from the hydrotreating of rapeseed oil with Pt/Zeolite and NiMo/Al<sub>2</sub>O<sub>3</sub> catalysts. *Ind. Eng. Chem. Res.* **2011**, *50*, 2791–2799.
22. Huber, G.W.; O'Connor, P.; Corma, A. Processing biomass in conventional oil refineries: Production of high quality diesel by hydrotreating vegetable oils in heavy vacuum oil mixture. *Appl. Catal. A* **2007**, *329*, 120–129.
23. Liu, Y.; Sotelo-Boyás, R.; Murata, K.; Minowa, T.; Sakanishi, K. Hydrotreatment of Jatropha oil to produce green diesel over trifunctional Ni-Mo/SiO<sub>2</sub>-Al<sub>2</sub>O<sub>3</sub> catalyst. *Chem. Lett.* **2009**, *38*, 552–553.
24. Liu, Y.; Sotelo-Boyás, R.; Murata, K.; Minowa, T.; Sakanishi, K. Hydrotreatment of vegetable oils to produce bio-hydrogenated diesel and liquefied petroleum gas fuel over catalysts containing sulfided Ni-Mo and oil acids. *Energy Fuel* **2011**, *25*, 4675–4685.
25. Nagai, M.; Koizumi, K.; Omi, S. NH<sub>3</sub>-TPD and XPS studies of Ru/Al<sub>2</sub>O<sub>3</sub> catalyst and HDS activity. *Catal. Today* **1997**, *35*, 393–405.
26. Mott, C.J.B. Clay minerals—An introduction. *Catal. Today* **1988**, *2*, 199–208.
27. Klopogge, J.T. Synthesis of smectites and porous pillared clay catalysts: A review. *J. Porous Mater.* **1998**, *5*, 5–41.
28. Martinez-Ortiz, M.J.; Fetter, G.; Dominguez, J.M.; Melo-Banda, J.A.; Ramos-Gomez, R. Catalytic hydrotreating of heavy vacuum gas oil on Al- and Ti-pillared clays prepared by conventional and microwave irradiation methods. *Micropor. Mesopor. Mater.* **2003**, *58*, 73–80.
29. Liu, Y.; Murata, K.; Okabe, K.; Inaba, M.; Takahara, I.; Hanaoka, T.; Sakanishi, K. Selective hydrocracking of Fischer-Tropsch waxes to high-quality diesel fuel over Pt-promoted polyoxocation-pillared montmorillonites. *Top. Catal.* **2009**, *52*, 597–608.
30. Bunch, A.Y.; Wang, X.; Ozkan, U.S. Hydrodeoxygenation of benzofuran over sulfided and reduced Ni-Mo/γ-Al<sub>2</sub>O<sub>3</sub> catalyst: Effect of H<sub>2</sub>S. *J. Mol. Catal. A* **2007**, *270*, 264–272.
31. Klopogge, J.T.; Welters, W.J.J.; Booy, E.; de Beer, V.H.J.; van Santen, R.A.; Geus, J.W.; Jansen, J.B.H. Catalytic activity of nickel sulfide catalysts supported on Al-pillared montmorillonite for thiophene hydrodesulfurization. *Appl. Catal. A* **1993**, *97*, 77–85.
32. Iranmahboob, J.; Toghiani, H.; Hill, D.O. Dispersion of alkali on the surface of Co-MoS<sub>2</sub>/clay catalyst: A comparison of K and Cs as a promoter for synthesis alcohol. *Appl. Catal. A* **2003**, *247*, 207–218.

33. Liu, Y.; Murata, K.; Hanaoka, T.; Inaba, M.; Sakanishi, K. Syntheses of new peroxo-polyoxometalates intercalated layered double hydroxides for propene epoxidation by molecular oxygen in methanol. *J. Catal.* **2007**, *248*, 277–287.
34. Liu, Y.; Murata, K.; Sakanishi, K. Hydroisomerization-cracking of gasoline distillate from Fischer–Tropsch synthesis over bifunctional catalysts containing Pt and heteropolyacids. *Fuel* **2011**, *90*, 3056–3065.
35. Liu, Y.; Koyano, G.; Misono, M. Hydroisomerization of *n*-hexane and *n*-heptane over platinum-promoted Cs<sub>2.5</sub>H<sub>0.5</sub>PW<sub>12</sub>O<sub>40</sub> (Cs2.5) studied in comparison with several other solid acids. *Top. Catal.* **2000**, *11*, 239–246.
36. Liu, Y.; Na, K.; Misono, M. Skeletal isomerization of *n*-pentane over Pt-promoted cesium hydrogen salts of 12-tungstophosphoric acid. *J. Mol. Catal. A* **1999**, *141*, 145–153.
37. Liu, Y.; Misono, M. Hydroisomerization of *n*-butane over platinum-promoted cesium hydrogen salt of 12-tungstophosphoric acid. *Materials* **2009**, *2*, 2319–2336.

© 2012 by the authors; licensee MDPI, Basel, Switzerland. This article is an open access article distributed under the terms and conditions of the Creative Commons Attribution license (<http://creativecommons.org/licenses/by/3.0/>).